

**SCP-2/SCP-x GENE ABLATION IMPACTS BRANCHED-CHAIN LIPID
HOMEOSTASIS**

An Undergraduate Research Scholars Thesis

by

KIMBERLY HEIN

Submitted to the Undergraduate Research Scholars program
Texas A&M University
in partial fulfillment of the requirements for the designation as an

UNDERGRADUATE RESEARCH SCHOLAR

Approved by
Research Advisor:

Dr. Ann Kier

May 2016

Major: Biomedical Sciences

TABLE OF CONTENTS

	Page
ABSTRACT.....	1
DEDICATION.....	2
ACKNOWLEDGEMENTS.....	3
NOMENCLATURE.....	4
CHAPTER	
I INTRODUCTION.....	6
Objectives.....	8
II METHODS.....	9
III RESULTS.....	15
Cholesterol Homeostasis.....	15
Cholesterol Branched-Side Chain Oxidation to Bile Acids Facilitates Intestinal Uptake and Hepatic Biliary Excretion of Branched-chain lipids (Cholesterol, Phytanic acid).....	19
Phytanic Acid Homeostasis.....	23
Fatty Acid Level.....	23
IV CONCLUSION.....	26
Cholesterol Homeostasis.....	26
Fatty Acid Homeostasis.....	27
REFERENCES.....	29

ABSTRACT

SCP-2/SCP-x Gene Ablation Impacts Branched-Chain Lipid Homeostasis

Kimberly Hein
Department of Veterinary Medicine and Biomedical Sciences
Texas A&M University

Research Advisor: Dr. Ann Kier
Department of Veterinary Pathobiology

Phytanic acid is one of many branched-chained fatty acids that humans and animals consume on a daily basis, but impaired metabolism of this compound and other branched-chain lipids such as cholesterol leads to toxicity. This toxicity may cause a variety of metabolic disruptions, but the full mechanism behind the branched-chain lipid accumulation has not been discovered. Additionally, phytanic acid binds to receptors similarly to fibrates, less toxic drugs developed from branched chain fatty acids like phytanic acid, which are used for controlling high triglycerides and cholesterol. Thus, errors in phytanic acid processing can cause similar problems in fibrate processing. *In vitro* studies showed that Sterol Carrier Protein-2 (SCP-2) and Sterol Carrier Protein-x (SCP-x), encoded by the same *Scp-2* gene through different initiation sites, facilitate branched-chain lipid metabolism. Since their physiological impact is not yet clear, SCP-2/SCP-x gene ablated (“double knockout”, DKO) and wild-type mice were fed control versus high phytol diet. Lipid analysis, real-time PCRs and western blotting of livers and serum demonstrated that SCP-2/SCP-x markedly impact branched-chain lipid metabolism—leading to cholesterol and lipid accumulation.

DEDICATION

Dedicated to my family whose support was crucial to my success.

ACKNOWLEDGMENTS

The assistance of Danilo Landrock and Drs. Ann Kier, Friedhelm Schroeder, Gregory Martin, Avery McIntosh, Kerstin Landrock, Huan Huang, and Sherrelle Milligan during this project is gratefully acknowledged.

NOMENCLATURE

SCP-2	Sterol Carrier Protein-2
SCP-x	Sterol Carrier Protein-x
DKO	SCP-2/SCP-x double gene ablated, Double Knock-Out (DKO)
PPAR α	Peroxisome Proliferator-Activated Receptor Alpha
WT	Wild Type
<i>Srebf2</i>	<i>Sterol Regulatory Element Binding Factor 2</i>
SREBP2	Sterol Regulatory Element-Binding Protein2
HMGCR	HMG-CoA Reductase
HMGCS1	HMG-CoA Synthase
ABCG5	ATP-Binding Cassette, Sub-Family G (WHITE), Member 5
ABCG8	ATP-Binding Cassette, Sub-Family G (WHITE), Member 8
MTP (<i>Mtp</i>)	Microsomal Triglyceride Transfer Protein
<i>Scarb1</i>	<i>Scavenger receptor class b member 1</i>
<i>Ldlr</i>	<i>LDL receptor</i>
<i>Soat2</i>	<i>Sterol O-Acyltransferase2</i>
<i>Lipe</i>	<i>Lipase</i>
<i>Cyp7a1</i>	<i>Cholesterol 7-Alpha-Hydroxylase or Cytochrome P450, Family 7, Subfamily A, Polypeptide 1</i>
<i>Cyp27a1</i>	<i>Cholesterol 27-Alpha-Hydroxylase or Cytochrome P450, Family 7, Subfamily A, Polypeptide 1</i>
<i>Acox2</i>	<i>Acyl-CoA Oxidase 2, Branched Chain</i>
<i>Srebf1</i>	<i>Sterol Regulatory Element Binding Transcription Factor 1</i>

ACC-1	Acetyl-CoA Carboxylase Alpha
ACC-2	Acetyl-CoA Carboxylase Beta
FASN	Fatty acid synthase
<i>Cpt1a</i>	<i>Carnitine Palmitoyltransferase 1a</i>
<i>Cpt2</i>	<i>Carnitine Palmitoyltransferase 2</i>
<i>Ppara</i>	<i>Peroxisome Proliferator-Activated Receptor Alpha</i>
<i>Oatp1</i>	<i>Ornithine Aminotransferase Pseudogene 1</i>
<i>Oatp2</i>	<i>Ornithine Aminotransferase Pseudogene 2</i>
NTCP	Na/Taurocholate Cotransporting Polypeptide
<i>SLC10A1</i>	<i>Solute Carrier Organic Anion Transporter Family, member 1a1 (Sodium/Bile Acid Cotransporter), Member 1</i>
ABCB11	ATP-Binding Cassette, Sub-Family B (MDR/TAP), Member 11
ABCB4	ATP-Binding Cassette, Sub-Family B (MDR/TAP), Member 4
LFABP	Liver-Type Fatty Acid Binding Protein (FABP1)

CHAPTER I

INTRODUCTION

Every day animals and humans alike consume fatty acids like phytanic acid. Phytanic acid is found in high abundance in dairy products. During digestion, bacteria in the ruminant intestine cleave chlorophyll's side chains, producing phytol, which is then converted into phytanic acid. The average for human consumption is 50-100 mg/day of phytanic acid¹. Inborn errors in phytanic acid metabolic degradation cause diseases such as the genetic condition Refsum's disease. This condition, resulting from phytanic acid accumulation in tissues rather than being metabolized, causes toxicity, inflammation, other lesions and death. Phytanic acid accumulation also contributes to the symptoms of peroxisomal biogenesis disorders and rhizomelic chondrodysplasia puncta type 1, death of astrocytes, and heart lesions². On the other hand, phytanic acid binds to the same receptors as fibrates³. Fibrates are common lipid-lowering drugs prescribed to control high triglyceride and cholesterol. Both fibrates and phytanic acid activate the nuclear hormone receptor peroxisome proliferator-activated receptor alpha (PPAR α)³. Fibrates such as clofibrate were developed to replace phytanic acid, and act as a less toxic treatment analog⁴.

Depending upon concentration, phytanic acid accumulation can cause rapid liver and cardiac necrosis and death in SCP-2/SCP-x gene-ablated (DKO) mice⁵. Sexual dimorphic differences in SCP-x and SCP-2 expression contribute to how quickly the toxicity is reached⁵. Phytanic acid is processed in several steps, first outside of peroxisomes, where phytol is converted into phytanic acid and then into phytanoyl-CoA by phytanoyl-CoA ligase². The phytanoyl-CoA is then

transported across the peroxisome's membrane where it undergoes alpha oxidation, followed by beta oxidation⁶. During alpha oxidation in the peroxisomes, one carbon (carboxyl terminal) is removed, turning phytanic to pristanic acid⁶. Pristanic acid is then broken down further in several beta oxidative steps (dehydrogenation, hydration, dehydration, thiolytic cleavage) in the peroxisome and converted into a much-shortened medium chain fatty acid⁶. The medium chain fatty acid then diffuses out of the peroxisome into the cytosol, diffuses into mitochondria since it bypasses transporters required for long chain fatty acid translocation across the mitochondrial membrane, and is further oxidized into carbon dioxide and water in mitochondrial matrix⁶. Previous research in our lab produced SCP-2/SCP-x double gene ablated mice. The *Scp-2* gene, which codes for both SCP-2 and SCP-x in 2 transcription sites, was ablated (double knock-out, DKO). This gene has a significant role in beta oxidation of branched-chain fatty acids².

Previous to my project, wild type (WT) and DKO C57Bl/6N male and female mice were fed a 0.5% phytol diet versus a phytol-free control diet. Throughout the study, mouse body weights and food consumptions were measured every second day, and at necropsy, liver weights were obtained. In the phytol-fed DKO mice, liver lipid levels, phospholipid, total cholesterol, and cholesteryl ester levels increased, with the percent change dependent upon the sex of the mouse, i.e., sexual dimorphism. These results indicated that lack of these two key fatty acid binding proteins significantly affected lipid metabolic pathways. My research project expanded upon the previous work, through the use of quantitative polymerase chain reactions to measure RNA expression, and western blotting to measure protein quantities in potentially affected genes of lipid metabolic pathways.

Objectives

The major goals for my research are to understand how SCP-2/SCP-x gene ablation impacts branched-chain lipid metabolism and accumulation, and in particular which proteins, enzymes and nuclear receptors are affected. Through this research and the knowledge gained therein, a better understanding of genetic errors in branched-chain lipid metabolism will be gained. Longer term impact will be to facilitate development of improved pharmaceuticals for treating high cholesterol, hypertriglyceridemia, and other conditions with less toxicity and fewer side effects.

CHAPTER II

METHODS

Animals All animal research used protocols that were first approved by the Institutional Animal Care and Use Committee at Texas A&M University. *Scp-2* gene ablated (DKO) mice were produced as described previously in the lab.⁷ Wild-type (WT) C57Bl/6N male and female mice of 6 weeks of age and weighing 20-30g at the beginning of this study were obtained from the National Cancer Institute (Frederick Cancer Research and Developmental Center, Frederick, MD). DKO male and female congenic mice were bred in-house to the same age and weight. The mice were fed a standard rodent chow mix until the beginning of the dietary study, and all mice were kept under a 12:12-h light-dark cycle in a 25° C temperature controlled facility. Water was available *ad libitum*, and mice were monitored by sentinels quarterly for infectious diseases. Western blotting of WT and DKO mouse livers confirmed the complete absence of SCP-2 and 58 kDa SCP-x, as well as the 43 kDa SCP-x cleavage product (Figs.1, 2, and 3).

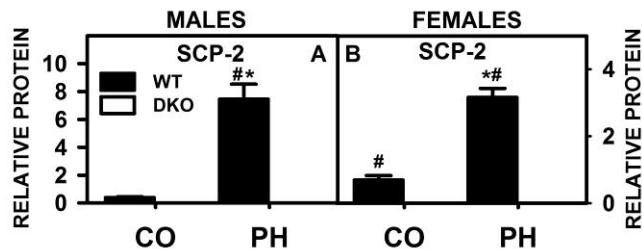


Fig. 1. Relative protein levels of SCP-2 determined in male and female SCP-2/SCP-x DKO and WT mice on control or 0.5% phytol diet. Mean \pm SE n=5-7 animals per group. * $p < 0.05$ between animals of same feeding group; # $p < 0.05$ on animals with same genotype but different feeding group.

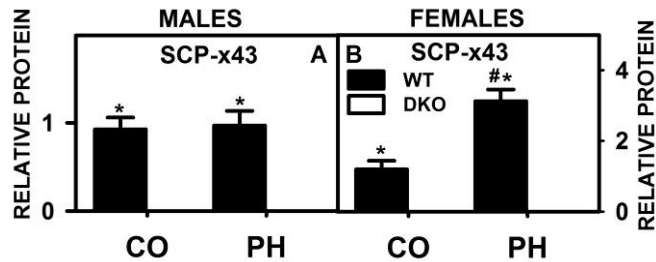


Fig. 2. Relative protein levels of SCP-x at the 43 kDa band determined in male and female SCP-2/SCP-x DKO and WT mice on control (CO) or 0.5% phytol (PH) diet. Mean \pm SE n=5-7 animals per group. * p < 0.05 between animals of same feeding group; # p < 0.05 on animals with same genotype but different feeding group.

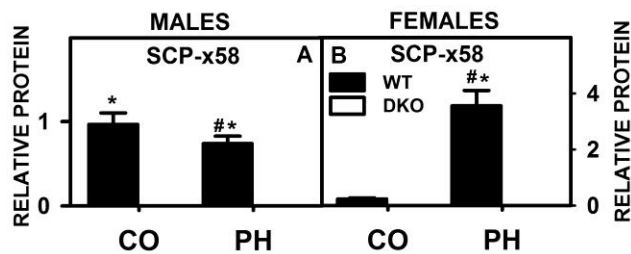


Fig. 3. Relative protein levels of SCP-x at the 58 kDa band determined in male and female SCP-2/SCP-x DKO and WT mice on control or 0.5% phytol diet. Mean \pm SE n=5-7 animals per group. * p < 0.05 between animals of same feeding group; # p < 0.05 on animals with same genotype but different feeding group.

Phytol dietary experiment Male and female mice of 6 weeks 20-30g were switched to a modified AIN-76A phytol-free, phytoestrogen-free rodent diet (diet no. D11243, Research Diets, New Brunswick, NJ) one week prior to the start of the dietary experiment. This process was to allow for standardization of phytol levels in the mice, as normal rodent chow mix includes phytanic acid and phytol of varying quantities. Each mouse was housed individually in Techniplast Sealsafe IVC cages. One half of the mice were then moved to a modified AIN-76 rodent diet supplemented with 0.5% phytol, (diet no. D01020601, Research Diets) while the other half remained on the phytoestrogen-free diet. The weights of the mice were monitored every other day at a consistent time, and food pellets were collected and weighed to monitor consumption. At the end of the study, mice were fasted overnight and anesthetized for blood collection via cardiac puncture (100mg/kg ketamine and 10 mg/kg xylaxine). Mice were then humanely euthanized and livers were harvested and weighed. Livers and all other major organs were snap frozen with dry ice. Small portions were also placed in RNAlater (Ambion, Austin, TX) and snap

frozen for RNA isolations. In WT, but not DKO, mice dietary phytol induced the hepatic expression of SCP-2 more so in male mice than females, but induced higher expression of both 58 and 43 kDa SCP-x in females than males (Fig. 1-3).

Serum, liver, and bile collection and lipid analysis The analysis and collection was performed as described previously in the lab⁸. The collected blood was stored at 4°C overnight and centrifuged for 20 minutes at 20,000 xg to isolate and prepare the serum. The serum was then stored at -80°C. Gall bladders and bile within were dissected from the livers and also stored at -80°C. Portions of the livers from each mouse (about 0.1g net weight) were homogenized in homogenate buffer containing 250mM sucrose, 10mM Tris-HCl and one protease inhibitor cocktail tablet (Cat. # 1836153, Roche) for 5 minutes at 1,500 rpm with a motor-driven pestle (Tekmar, Cincinnati, OH). After homogenization the samples were centrifuged at 200 xg for 5 minutes. The supernatant was collected and analyzed for protein levels. The protein levels of the liver homogenate and the serum were determined via Bradford micro-assay from Bio Rad laboratories (cat no. 500-0006; Hercules, CA). For the various assays, 96 well assay plates (Corning, Corning; NY) and a Bio Tek Synergy 2 microplate reader (Bio Tek Instruments, Winooski, VT) were used. Wako diagnostic kits (Richmond, VA) were used to quantify the total cholesterol, free cholesterol, triglyceride, and phospholipid levels in the serum and liver homogenate. The total bile acids for the serum and liver were quantified using the Diazyme Kit (Poway, CA). All the commercially available kits were performed via manufacturer's instructions modified for use with 96-well plates and the microreader mentioned above.

Western blotting Protein translation product levels were determined by western blotting analysis. Livers were homogenized following the process detailed above and centrifuged at 200 xg for 5 minutes and the supernatant collected. The protein levels of this supernatant were again analyzed by Bradford micro-assay form Bio-Rad-Laboratories (cat. No. 500-0006; Hercules, CA). The samples were then mixed with 2x sample loading buffer (1:1 v/v) containing 1.6M glycerol, 0.3M SDS, 0.1M Tris-HCl, 0.6M 2-mercaptoethanol, and Coomassie Brilliant Blue G-250. The samples were then heat denatured at 95°C for 5 minutes and briefly centrifuged. As the proteins of interest were separated from a housekeeper COX IV on the 12% polyacrylamide gels, the membranes were cut into separate pieces so that the protein loading of the target protein could be compared to a standard. The samples underwent SDS-page separation on polyacrylamide gels run at 150V till visual separation had occurred (3-3.5 hours) and were transferred onto nitrocellulose membranes (162-0112, Bio-Rad, Hercules, CA). The transfer process occurred for 2 hours at 500mA on ice using a transfer buffer that contains 0.2M glycine and 12.5 mM Tris base in 20% methanol. To confirm protein transfer, Ponceau staining was performed (P7170, Sigma-Aldrich, St. Louis, MO). The membranes were incubated in 3% gelatin for one hour prior to the addition of the primary antibody to reduce nonspecific antibody binding. The primary antibody was incubated overnight at room temperature with gentle shaking. The primary antibody was in TBST (10 mM Tris-HCl pH 8.0, 150 mM NaCl, and 0.05% tween 20) and 1% gelatin. Secondary antibodies of alkaline-phosphatase conjugates of the anti-goat, anti-rabbit or anti-mouse IgG (Sigma) in TBST and 1% gelatin were used. The secondary antibody was incubated on the membranes for 1-2 hours at room temperature with a gentle shaker. After removal of the secondary the membranes were washed 3x5min with TBST, and then washed with alkaline phosphatase buffer which contains 100mM Tris-HCl (ph9.0), 100mM NaCl, and 5

mM MgCl₂. The color development was developed by the addition of alkaline phosphatase substrate and premixed with Sigma Fast 5-bromo-4-chloro-3-indoyl phosphate/nitroblue tetrazolium tablets (BCIP/NBT; Sigma) to the previously primary and secondary antibody incubated membranes. The readings were quantified through using a scanner (Epson Perfection V700 Photo Scanner) and a computer workstation. ImageJ analysis software (version 1.48, Wayne Rasband, National Institutes of Health, Bethesda, MD) was used to analyze the image files (mean 8-bit grayscale density). The protein expression levels were normalized to the housekeeper standard mean expression. The analyzed band intensities were then compared through standard curves and to quantify changes in protein expression.

Quantitative Real-time PCR Real time PCR was performed on isolated total RNA from livers stored in a stabilizing buffer and purified following the manufacturers protocol via an RNeasy minikit (Qiagen, Valencia, CA). RNA concentrations were then determined spectrophotometrically. For real time quantitative PCR (qRT-PCR) measurements, an ABI PRISM 7000 Sequence Detection System (Applied Biosystems, Foster City, CA) was used to analyzed expression patterns, using a TAqMan One Step PCR Master Mix Reagent kit, the thermocycler cycled 50°C for 10 min, 95°C for 3 min, and 40 repetitions of 95°C for 0:15 min and 60°C for 1 min. Different assays were used to identify expression profiles of specific mRNAs. The expression profiles were normalized to an internal reference standard (18S rRNA) and were analyzed using the ABI PRISM 7000 SDS software. The male samples were made relative to the control diet WT male mice, while the females were made relative to the control diet WT female mice.

Analysis Each group contained five to seven animals, and all values expressed as mean \pm standard error (SE). Statistics were performed using ANOVA with a Newman-Keuls multiple comparisons test (GraphPad Prism, San Diego, CA). Statistical significance was established at $p < 0.05$. For all western blot and PCR data, the males were normalized to the WT control diet males and the females to the WT control diet females. In the lipid analysis, all mice were normalized to the WT control diet males.

CHAPTER III

RESULTS

Cholesterol Homeostasis

The SCP-2/SCP-x gene plays important roles in the branched-chain oxidation of both the branched-side chain of cholesterol as well as the branched-chain of phytanic acid. To determine the overall effects of the SCP-2/SCP-x gene ablation (DKO) and high phytol diet on hepatic and serum lipids, liver lipid analysis and serum analysis was performed as detailed in the Methods. Those lipids key to cholesterol homeostasis are shown below. Total liver lipids included cholesterol plus all other lipids the hepatocyte contains, while total cholesterol only included cholesterol. Free cholesterols are not esterified or bound to membranes, while cholesteryl esters are esterified. Total liver lipids, total and free cholesterol, and cholesterol ester were increased in both males and females in both the phytol and DKO mice as compared to controls (Fig 4). In serum, total cholesterol and cholesteryl ester was decreased in males and females both in phytol and DKO mice as compared to controls, while free cholesterol increased in both sexes for the DKO phytol mice (Fig. 5).

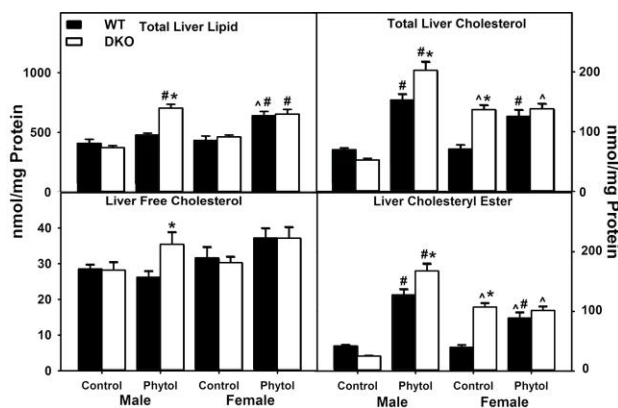


Fig. 4. Total levels of liver lipids determined in male and female SCP-2/SCP-x DKO and WT mice on control or 0.5% phytol diet. Mean \pm SE, $n=5-7$ animals per group. * $p < 0.05$ between mice of same feeding group; # $p < 0.05$ on animals with same genotype but different feeding group; ^ $p < 0.05$ on animals with same genotype and feeding group but different sex



Fig. 5. Total levels of serum lipids in male and female SCP-2/SCP-x DKO and WT mice on control or 0.5% phytol diet. Mean \pm SE, n=5-7 animals per group. * p <0.05 between mice of same feeding group; # p <0.05 on animals with same genotype but different feeding group.

To determine the effect of the SCP-2/SCP-x gene ablation (DKO) on cholesterol homeostasis, qRT-PCRs and western blotting were performed according to the protocol described in Chapter II. Cholesterol biosynthesis is affected by the transcription of *Srebf2*, as the protein transcribed by this transcript, SREBP2, is released from the endoplasmic reticulum under conditions of low cholesterol whereupon it traffics into the nucleus to induced transcription of other genes involved in *de novo* cholesterol biosynthesis such as *Hmgcr* and *Hmgcs1*. The rate-determining step in *de novo* cholesterol synthesis is controlled by HMG-CoA reductase (HMGCR, the protein translation product of *Hmgcr*) followed by further processing of HMG-CoA by HMG-CoA synthase (HMGCS1, protein translation product of *Hmgcs1*). In both males and females, there was a significant increase in transcription in the DKO phytol diet ($p < 0.05$, Fig. 6A-F). In males, all genes increased \sim 4-fold as compared to the WT control diet mice, but in females, the increase was more variable: *Srebf2* increased 2-fold, *Hmgcr* increased by 1.5-fold, and *Hmgcs1* by 2.5-fold. In comparison to genotype, the DKO control diet males increased in transcription but not significantly, while in females there was significant genotype effect ($p < 0.05$, Fig. 6D-F).

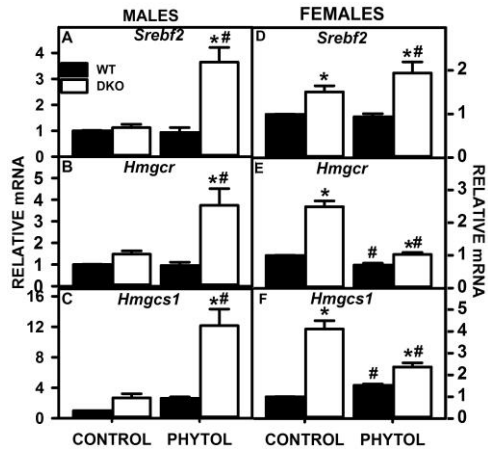


Fig. 6. Relative expression levels of key cholesterol biosynthesis enzymes in male and female SCP-2/SCP-x DKO and WT mice on control or 0.5% phytol diet. Mean \pm SE, n=5-7 animals per group. * p <0.05 between mice of same feeding group; # p <0.05 on animals with same genotype but different feeding group.

Cholesterol efflux and intracellular transport is accomplished through three key membrane proteins: ABCG5 and ABCG8 are ATP binding cassettes that promote excretion of cholesterol sterols into bile (*Abcg5* and *Abcg8*), while MTP (*Mttp*) is key in exporting cholesterol as VLDL. In males, ABCG5 displayed no significant increase in expression (Fig 7A). Females had a small, but significant reduction of expression in the WT phytol diet mice as compared to the WT control diet mice, and a significant increase in expression of the DKO phytol diet mice when compared to the WT phytol (Fig 7D). For ABCG8, the DKO control diet males had a significant increase in expression when compared to the WT control diet males (Figure 7B). In females, the WT phytol diet mice had a significant decrease in expression when compared to the WT control diet mice and the DKO phytol diet mice had a significant increase when compared to the WT phytol diet mice (Figure 7E). In *Mttp*, there was a nearly 6-fold increase in the DKO phytol diet males, which was a significant increase in expression when compared to the WT control diet and WT phytol diet males (Figure 7C). In females, there was a significant increase in expression of the DKO control diet mice and the WT phytol diet mice compared to the WT control diet mice (Fig. 7F).

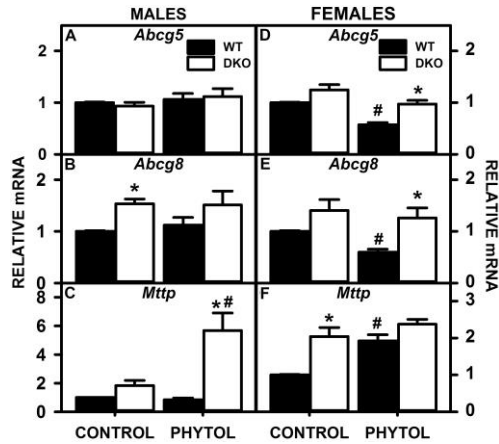


Fig. 7. Relative expression levels of key cholesterol efflux and intracellular transport enzymes determined in male and female SCP-2/SCP-x DKO and WT mice on control and 0.5% phytol diet. Mean \pm SE, n=5-7 animals per group. * p <0.05 between animals of same feeding group; # p <0.05 on animals with same genotype but different feeding group

In cholesterol uptake and esterification, *Scarb1*, *Ldlr*, *Soat2*, and *Lipe* transcribe key enzymes. *Scarb1* transcript encodes the protein responsible for HDL binding and being taken into the cell. *Ldlr* encodes for the LDL receptor. *Soat2* encodes for ACAT2, which converts long chain cholesterol into cholesterol esters using fatty acyl CoAs. *Lipe* converts cholesterol esters into cholesterol. For *Scarb1*, the males had no significant increase in expression (Fig 8-A), while the females had an upregulation in the DKO control and phytol diet mice, but only the DKO control diet mice were of a significant value (Fig 9-A). *Ldlr* in both male and female mice had an increase in expression of the DKO control and phytol diet mice. While the female values were both significant for their feeding groups, only the male DKO phytol diet mice was of significance (Fig 8-B, 9-B). In the males only, the DKO phytol had a significant increase in expression of *Soat2* when compared to the WT control and phytol mice (Fig 8-C). DKO females on the control diet had a significant increase in expression of *Soat2* compared to the WT control diet mice and phytol diet mice were increased in expression when compared to the control diet mice (Fig 9-C). *Lipe* in males had no significant increase in expression, while the females had a significant increase in the DKO control diet when compared to the WT control diet and the DKO phytol diet mice (Fig 8-D, 9-D).

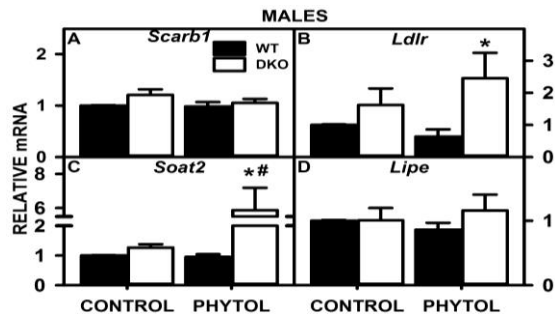


Fig 8. Relative expression levels of key cholesterol uptake and esterification enzymes in male SCP-2/SCP-x DKO and WT mice on control and 0.5% phytol diet. Mean \pm SE, n=5-7 animals per group * p < 0.05 between mice of same feeding group; # p < 0.05 on animals with same genotype but different feeding group.

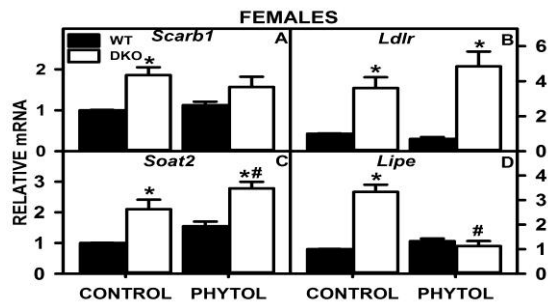


Fig 9. Relative expression levels of key cholesterol uptake and esterification enzymes determined in female SCP-2/SCP-x DKO and WT mice on control and 0.5% phytol diet. Mean \pm SE, n=5-7 animals per group * p < 0.05 between mice of same feeding group; # p < 0.05 on animals with same genotype but different feeding group.

Cholesterol Branched-Side Chain Oxidation to Bile Acids Facilitates Intestinal Uptake and Hepatic Biliary Excretion of Branched-chain lipids (Cholesterol, Phytanic acid)

Both intestinal absorption as well as hepatic biliary excretion require the presence of bile acids derived by hepatic metabolism of cholesterol's branched side chain. Essential in bile acid synthesis are *Cyp7a1* and *Cyp27a1*, genes encoding the key enzymes that are rate-limiting in the primary and secondary pathways of cholesterol branched side-chain oxidation for initiating bile acid synthesis. While both enzymes oxidize cholesterol for bile acid synthesis, *Cyp7a1* catalyzes the primary pathway for bile acid synthesis. In males, *Cyp7a1* was significantly increased in expression for the DKO control diet, WT phytol diet, and DKO phytol diet mice as compared to the WT control diet mice (Fig 10-A). The DKO phytol diet mice are also significantly increased in expression when compared to the DKO control diet mice (Fig 10-A). In females, the DKOs

are increased in expression compared to the WT mice, and the DKO phytol diet mice were down expressed compared to the DKO control diet mice (Fig. 10-C). For *Cyp27a1*, rate limiting in the secondary bile acid synthetic pathway, expression was significantly increased in male DKO phytol mice as compared the WT control diet mice (Fig 10-B) as well as in females, regardless of diet (Fig. 10-D).

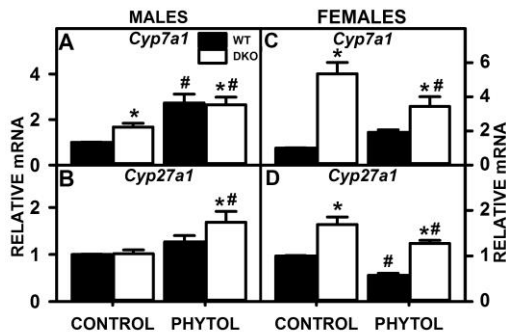


Fig 10. Relative expression levels of key cholesterol oxidation enzymes determined in male and female SCP-2/SCP-x DKO and WT mice on control or 0.5% phytol diet. Mean \pm SE, n=5-7 animals per group. * $p < 0.05$ between animals of same feeding group; # $p < 0.05$ on animals with same genotype but different feeding group.

The net effect on liver total bile acid levels was determined. In males, bile acid levels increased in the WT phytol diet mice, and significantly decreased in DKO phytol diet mice, while in the DKO mice, levels remained unchanged (Fig. 11). The female control diet mice had significantly greater levels than male control diet mice, and the female phytol diet mice had greatly reduced levels when compared to the control diet mice (Fig. 11)

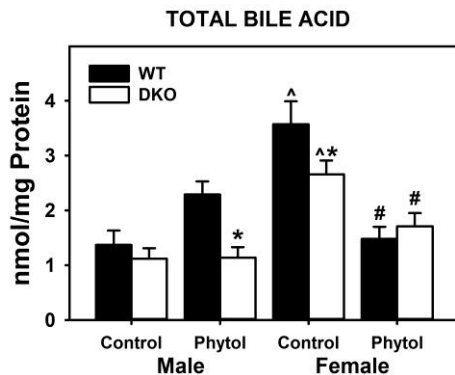


Fig. 11. Total levels of bile Acids determined in male and female SCP-2/SCP-x DKO and WT mice on control or 0.5% phytol diet. Mean \pm SE, n=5-7 animals per group. * $p < 0.05$ between mice of same feeding group; # $p < 0.05$ in animals with same genotype but different feeding group; ^ $p < 0.05$ between animals with same genotype and feeding group but different sex.

To determine if these differences were attributed only to loss of SCP-2/SCP-x or concomitant upregulation of other proteins/transporters in bile acid homeostasis, gene expression of the five key enzymes in bile acid uptake and excretion was examined. *Oatp1* and *Oatp2* genes code for bile salts transporters, while *Ntcp* (sodium/bile acid cotransporter) codes for a sodium and bile cotransporter that participates in the transport of bile acids. ABCB11, also known as BSEP, is a major bile export pump. ABCB4 also known as MDR3 or MDR2 transports phospholipids from liver hepatocytes to bile. *Oatp1* in the males had a significant down expression in the DKO phytol diet mice when compared to the DKO control diet mice and to the WT phytol diet mice, and a non-significant increase in the expression in the DKO control diet mice when compared to the WT control diet mice (Fig. 12-A). In females, there was a significant up regulation in the DKO diet mice when compared to the WT mice, and significant down regulation of the phytol diet mice in control diet mice (Fig.13-A). *Oatp2* in the males significantly decreased in the DKO mice when compared to their respective WT mice, and a significant decrease in the WT phytol diet mice when compared to the control diet WT mice (Fig. 12-B). The phytol females significantly decreased in expression when compared to the control diet mice, and while not significant, the DKO phytol diet mice were upregulated when compared to the WT phytol diet mice (Fig. 13-B). In males, both DKO groups were down regulated in *Ntcp* when compared to their respective WT mice, but were only significant in the DKO phytol diet mice, and the DKO phytol diet mice were significantly down expressed compared to the WT phytol diet mice (Fig. 12-C). In females, there was a significant increase in expression in the DKOs when compared to their respective control diet mice, and a significant decrease in expression of the phytol diet mice when compared to their respective control (Fig. 13-C). In males, there was a significant increase of *Abcb11* in DKO control diet mice when compared to the WT control diet mice, and a

significant increase in DKO control diet and WT phytol diet mice in comparison to the WT control diet mice, and a significant decrease in expression in *Abcb11* in the DKO phytol diet mice when compared to the WT control diet mice and the DKO control diet mice (fig. 12-D). In females, the DKO control diet mice was significantly increased in expression when compared to the WT control diet mice, and DKO phytol diet mice were significantly decreased in expression of *Abcb11* compared to DKO control diet mice (fig. 13-D). In males, there was a significant increase in expression of *Abcb4* in the DKO phytol diet mice in comparison to the DKO control diet and the WT phytol diet mice (Fig. 12-E). In females, the DKO phytol diet mice were significantly increased in expression of *Abcb4* when compared to the WT phytol diet mice and the DKO control diet mice (Fig. 13-E).

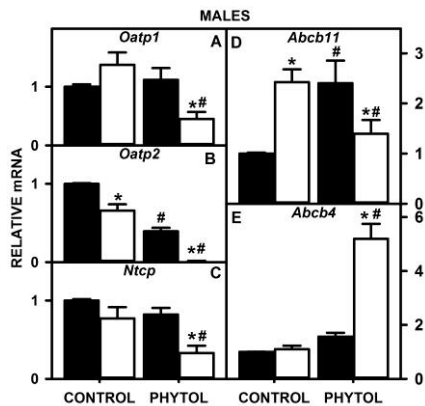


Fig. 12. Relative expression levels of key bile acid uptake and esterification enzymes determined in male SCP-2/SCP-x DKO and WT mice on control and 0.5% phytol diet. Mean \pm SE, n=5-7 animals per group * $p < 0.05$ between mice of same feeding group; # $p < 0.05$ on animals with same genotype but different feeding group.

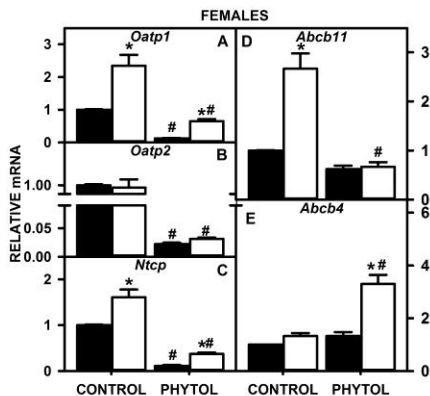


Fig. 13. Relative expression levels of key bile acid uptake and esterification enzymes determined in female SCP-2/SCP-x DKO and WT mice on control and 0.5% phytol diet. Mean \pm SE, n=5-7 animals per group * $p < 0.05$ between mice of same feeding group; # $p < 0.05$ on animals with same genotype but different feeding group.

Phytanic Acid Homeostasis

To determine if SCP-2/SCP-x gene ablation elicited compensatory upregulation of the other key enzyme in phytanic acid oxidation, expression levels of *Acox2*, the key peroxisomal enzyme in alpha-oxidation of phytanic acid's branched-chain, were determined. Phytol diet alone had little effect on expression of *Acox2* in WT mice (Fig. 14). In contrast, DKO significantly increased expression of *Acox2* in males fed phytol diet (Fig. 14-A). In the females, however, there was a significant increase of *Acox2* in DKO regardless of diet (Fig. 14-B). Despite upregulation of *Acox2*, however, DKO resulted in accumulation of phytol metabolites, especially phytanic acid (data not shown).

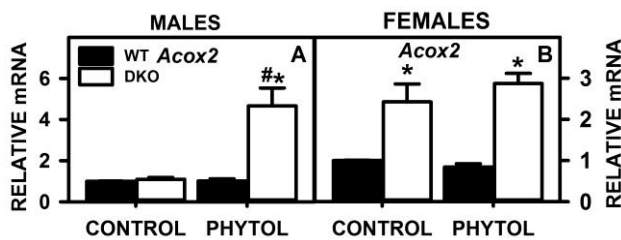


Fig 14. Relative expression levels of *Acox2* determined in male and female SCP-2/SCP-x DKO and WT mice on control or 0.5% phytol diet. Mean \pm SE n=5-7 animals per group. * p <0.05 between animals of same feeding group; # p <0.05 on animals with same genotype but different feeding group.

Fatty Acid Levels

Since impaired hepatic fatty acid uptake/metabolism elicits non-esterified fatty acid accumulation in serum, the impact of SCP-2/SCP-x gene ablation and dietary phytol on serum total non-esterified fatty acids was determined. There were some significant differences in several groups: in males the highest levels were found in the DKO phytol diet, while in the females the highest levels were in the WT phytol diet mice (Fig.15).

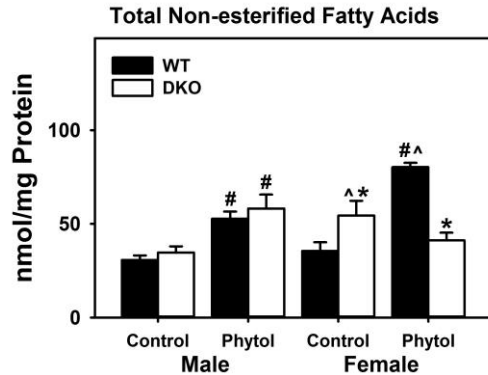


Fig. 15. Total levels of non-esterified fatty acids determined in male and female SCP-2/SCP-x DKO and WT mice on control or 0.5% phytol diet. Mean \pm SE, n=5-7 animals per group. * $p < 0.05$ between mice of same feeding group; # $p < 0.05$ on animals with same genotype but different feeding group; ^ $p < 0.05$ on animals with same genotype and feeding group but different sex.

To determine if these increases at least in part also reflected increased hepatic expression of proteins in *de novo* fatty acid synthesis were examined. This includes the key nuclear transcription factor *Srebf1* and its downstream target enzymes in such as acetyl-CoA carboxylase (*Acaca*, *Acacb*) and fatty acid synthase (*Fasn*) *Srebf1* encodes for SREBP1 which, under conditions of low cholesterol, is released from the endoplasmic reticulum, traffics into the nucleus, and becomes a nuclear transcription factor that binds to/activates the sterol regulatory element 1 (SREBP1) mediated transcription of genes involved not only in sterol biosynthesis, but also those in *de novo* fatty acid synthesis. ACC-1 (from *Acaca*) catalyzes the carboxylation of acetyl-CoA to malonyl-CoA in the rate limiting step in fatty acid synthesis. In contrast, ACC-2 (from *Acacb*) catalyzes the carboxylation of acetyl-CoA to malonyl Coa and plays a role in regulating fatty acid oxidation. Fatty acid synthase (from *Fasn*) catalyzes the synthesis of palmitate from acetyl-coA and malonyl CoA in the presence of NADPH into long chain fatty acids. In males and females on the DKO control diet, *Srebf1* was upregulated as compared to the WT control diet mice (Fig. 16-A and 17-A). While on the phytol diets, *Srebf1* was significantly down regulated compared to the control diet mice (Fig. 16-A and 17-A). *Acaca* in the males increased in the DKOs and in the phytol diet mice, with the greatest upregulation in the DKO phytol diet mice, but these increases were not significant (Fig 16-B). In females, there was a

significant increase in expression of *Acaca* in the DKO control diet mice, and a significant decrease in the phytol diet mice compared to the DKO control diet mice, and an upregulation in both DKOs compared to their respective WT mice (Fig. 17-B). In the males, *Acacb* was significantly upregulated in the DKOs and phytol diet mice (Fig. 16-C). In the females, there was a significant increase in expression in the DKO, while the DKO phytol mice were decreased in expression when compared to the DKO control diet mice (Fig. 17-C). In males, there was only a significant decrease of *Fasn* in the DKO phytol diet mice, but all the DKO expression was decreased compared to the WT, and there was an increase in expression in the phytol diet WT compared to the control diet WT mice (Fig. 16-D). In females, there was a significant decrease in the expression in both DKOs and the phytol diet mice (Fig. 17-D).

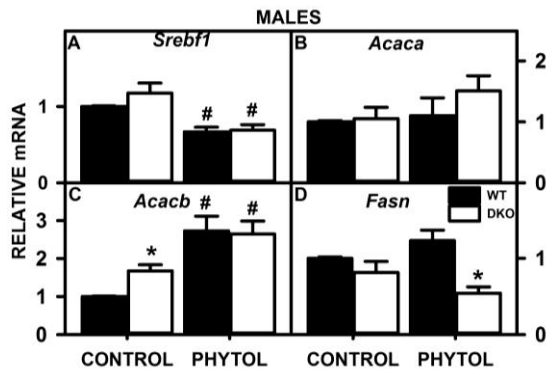


Fig. 16. Relative expression levels of key fatty acid synthesis enzymes determined in male SCP-2/SCP-x DKO and WT mice on control and 0.5% phytol diet. Mean \pm SE, n=5-7 animals per group * $p < 0.05$ between mice of same feeding group; # $p < 0.05$ on animals with same genotype but different feeding group.

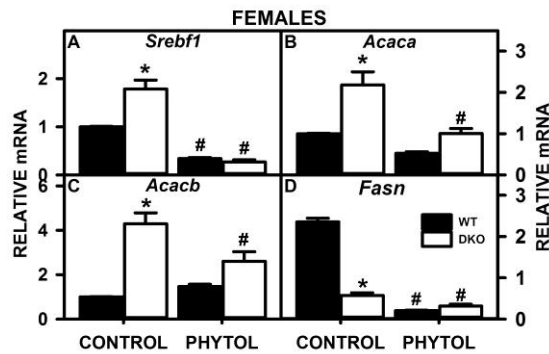


Fig. 17. Relative expression levels of key fatty acid synthesis enzymes determined in female SCP-2/SCP-x DKO and WT mice on control and 0.5% phytol diet. Mean \pm SE, n=5-7 animals per group * $p < 0.05$ between mice of same feeding group; # $p < 0.05$ with animals with same genotype but different feeding group.

CHAPTER IV

CONCLUSION

Cholesterol Homeostasis

SCP-x and SCP-2 have key roles in hepatic oxidation of branched-chain lipids such as phytanic acid and cholesterol.³ Dietary phytol competes with cholesterol for peroxisomal oxidation, leading to hepatic cholesterol accumulation (steatosis) in male and female mice (Fig. 4). Ablating SCP-2/SCP-x (DKO) also increased hepatic cholesterol accumulation by reducing peroxisomal oxidation of cholesterol's branched side chain to bile acids, thereby potentially reducing biliary cholesterol excretion and concomitantly decreasing cholesterol transfer to the ER which in turn increases SREBP2 release and induction of target enzymes in cholesterol synthesis, esterification, and secretion (Fig. 4, 5C, 5D, 6C, 6D). Effects of dietary phytol, SCP-2/SCP-x ablation, or both together on hepatic cholesterol phenotype are modified at least in part by the naturally lower levels of SCP-2 and SCP-x in females (mice and human). Cholesterol uptake and excretion are also increased in the DKO mice, particularly the females. These increases are due to the lack of cholesterol being transported to the endoplasmic reticulum (ER), causing the cell to release SREBP from the endoplasmic reticulum for trafficking to the nucleus and signaling for increased *de novo* cholesterol synthesis and uptake of more cholesterol. Since females naturally have lower levels of SCP-x and SCP-2, they process branched-chain lipids differently than males on a normal basis, as seen by the differences between in the control diet WT mice of both sexes in the lipid data (Fig. 1). This difference in SCP-x and SCP-2 and the resulting difference in metabolism, leads to the sexual dimorphism seen in the cholesterol homeostasis. Bile acid uptake and excretion is tied to cholesterol levels. Additionally normally

bile acid levels vary great between the sexes due to a natural sexual dimorphism. In the males the increase found in the WT phytol males, but not in the DKO phytol males indicates that in the presence of phytol, cholesterol levels rise causing bile acids to accumulate in the cell to be later excreted with the cholesterol, but without the SCP-2 chaperone the phospholipid transferring protein is increased to export the lipid accumulation into the bile. In the females the bile acid levels in the cell decrease in the presence of phytol as cholesterol accumulates the cell focuses on exporting it out of the cell in the bile, and the cells do not increase their uptake to counter act this excretion. In both sexes the liver cells are unable to uptake enough bile acid to transport all the accumulated cholesterol out of the cells and into the bile, leading to the accumulation of cholesterol in the cells seen above.

Fatty Acid Homeostasis

In WT mice, phytol increase non-esterified fatty acid levels and branched-chain oxidation (Figs. 15 and 14). In the WT mice phytol also decreases the expression of many *de novo* fatty acid synthesis mRNAs (Figs. 16 and 17). This implies that in the presence of large amounts of phytol, oxidation is increased in attempts to lower fatty acid levels before toxicity is increased, but the presence of phytol and its metabolites increases the total fatty acid levels in the hepatic cells. In the DKO mice on the control diet the fatty acid levels are increased and the branched-chain oxidation is increased in expression (Figs 14 and 15). The gene ablation of the mice on the control diet also increased the expression of all the *de novo* fatty acid synthesis mRNAs except *Fasn* which is decreased (Figs 16 and 17). This implies that due to the lack of the SCP-2 transporting the cholesterol to the ER the ER concentrations of cholesterol are decreased triggering the release of SREBP1. This release triggers to transcription of several *de novo* fatty

acid synthesis genes. While FASN is regulated by SREBP1 it is also regulated by LXR hence why its response differs from the rest of the fatty acid synthesis proteins.¹⁰ The SCP-2/SCP-x gene ablation modified the impacts of the phytol in several ways. First it augmented the increase in expression of the branch-chain oxidative mRNA (Fig. 14). This implies that in the absence of SCP-x the hepatic cell increases its *Acox2* expression in the presence of phytol in order to process it. Secondly in the males the combined effect increases fatty acid levels, while in the females it decreases fatty acid levels (Fig. 15). This indicates that the females' natural lower SCP-2/SCP-x level modifies their fatty acid homeostasis, and the further loss impacts the fatty acid levels greatly by potentially triggering other pathways. Thirdly the gene ablation has less of a modifying effect on the phytol impact on the *de novo* fatty acid synthesis (Figs. 16 and 17). This indicates that the high level of phytol impacts the levels of *de novo* fatty acid synthesis more than the gene ablation does.

Thus the gene ablation of SCP-2/SCP-x and a phytol diet greatly exacerbated hepatic lipid accumulation, particularly in cholesterol pathways, and as well impacted that of fatty acids (both branched-chain and normal straight-chain). These effects are influenced through sexual dimorphism, found both in human and mouse metabolism³. Currently this research seeks to aid in the understanding of the roles SCP-2 and SCP-x play in hepatic tissue branch-chain lipid metabolism, its roles in human lipid disorders, leading to new pharmaceutical targets for treatment.

REFERENCES

- 1) Atshaves B, McIntosh A, Lyuksyutova O, Zipfel W, Webbs W, Schroeder F. Liver Fatty Acid-binding Protein Gene Ablation Inhibits Branched-chain Fatty Acid Metabolism in Cultured Primary Hepatocytes. *J Biol Chem*. 2004 May; 279:30954-30965.
- 2) Wanders R, Komen J, Peroxisomes, Refsum's disease and the alpha- and omega-oxidation of phytanic acid. *J Biochem Soc Trans*, 2007 Jun; 35: 865-69.
- 3) Atshaves B, Payne R, McIntosh A, Tichy S, Russell D, Kier A, Schroeder F. Sexually dimorphic metabolism of branched-chain lipids in C57BL/6J mice. *J Lipid Res*, 2004 Mar;45:812-30.
- 4) Storey S, et al. Loss of intracellular lipid binding proteins differentially impacts saturated fatty acid uptake and nuclear targeting in mouse hepatocytes. *Am J Physiol*, 2012 Aug; 303: G837-G850.
- 5) Mönnig G, Wiekowski J, Kirchhof P, Stypmann J, Plenz G, Fabritz L, and et al. Phytanic acid accumulation is associated with conduction delay and sudden cardiac death in sterol carrier protein-2/sterol carrier protein-x deficient mice. *J Cardiovasc Electrophysiol* 2004 Nov; 15(11):1310-6.
- 6) Van den Brink D, Wanders R. Phytanic acid: production from phytol, its breakdown and role in human disease. *Cell Mol Life Sci*, 2006 June; 63: 1752-1765
- 7) Atshaves B, McIntosh A, Landrock D, Payne H, Mackie J, Maeda N, and et al. Effect of SCP-x gene ablation on branched-chain fatty acid metabolism. *Am J Physiol*. 2007 March; 292: 939-951.
- 8) Klipsic D, Landrock D, Martin GG, McIntosh AL, Landrock K, Macki J, and et al. Impact of *Scp-2/Scp-x gene ablation* and dietary cholesterol on hepatic lipid accumulation. *AM J Physiol*, 2015 September; 309(5): G387-G389
- 9) Petrescu AD, McIntosh AL, Storey SM, Huang H, Martin GG, et al. High glucose potentiates L-FABP mediated fibrate induction of PPARalpha in mouse hepatocytes. *Biochim Biophys Acta*. 2013 Aug; 1831(8): 1412-1425.
- 10) Horton JD, Goldstein JL, Brown MS. SREBPs: activators of the complete program of cholesterol and fatty acid synthesis in the liver. *J Clin Invest*. 2002 May; 109(9): 1125-1131.